

The Leaf Reticulate Mutant *dov1* Is Impaired in the First Step of Purine Metabolism

Christian Rosar^a, Kerstin Kanonenberg^a, Arun M. Nanda^{a,b}, Michael Mielewczik^{c,d}, Andrea Bräutigam^a, Ondřej Novák^e, Miroslav Strnad^e, Achim Walter^{c,d} and Andreas P.M. Weber^{a,e,1}

^a Institute for Plant Biochemistry, Heinrich-Heine-Universität, Universitätsstrasse 1, D-40225 Düsseldorf, Germany

^b Present address: Institute of Bio- and Geosciences, IBG-1: Biotechnology, Forschungszentrum Jülich, D-52425 Jülich, Germany

^c Institute of Bio- and Geosciences, IBG-2: Plant Sciences, Forschungszentrum Jülich, D-52425 Jülich, Germany

^d Present address: Institute of Agricultural Sciences, Universitätstrasse 2, ETH Zürich, CH-8092 Zürich, Switzerland

^e Laboratory of Growth Regulators, Palacky University & Institute of Experimental Botany AS CR, Slechtitelu 11, CZ-78371 Olomouc, Czech Republic

ABSTRACT A series of reticulated *Arabidopsis thaliana* mutants were previously described. All mutants show a reticulate leaf pattern, namely green veins on a pale leaf lamina. They have an aberrant mesophyll structure but an intact layer of bundle sheath cells around the veins. Here, we unravel the function of the previously described reticulated EMS-mutant *dov1* (differential development of vascular associated cells 1). By positional cloning, we identified the mutated gene, which encodes glutamine phosphoribosyl pyrophosphate aminotransferase 2 (ATase2), an enzyme catalyzing the first step of purine nucleotide biosynthesis. *dov1* is allelic to the previously characterized *cia1-2* mutant that was isolated in a screen for mutants with impaired chloroplast protein import. We show that purine-derived total cytokinins are lowered in *dov1* and crosses with phytohormone reporter lines revealed differential reporter activity patterns in *dov1*. Metabolite profiling unraveled that amino acids that are involved in purine biosynthesis are increased in *dov1*. This study identified the molecular basis of an established mutant line, which has the potential for further investigation of the interaction between metabolism and leaf development.

Key words: leaf development; reticulated mutants; cytokinin; growth kinetics; purine metabolism.

INTRODUCTION

Two different processes in leaf development can be distinguished: (1) the developmental program that governs leaf overall shape and size, and (2) the processes controlling internal leaf architecture. Schematically, all internal leaf tissues are wedged between two epidermal cell layers. In between, the mesophyll tissue harbors the photosynthetic activity. The mesophyll surrounds the vasculature that transfers solutes and water. During leaf development, at least in *Arabidopsis thaliana* (thale cress), the veins differentiate prior to the mesophyll because mesophyll differentiation precludes additional minor vein development (Pyke et al., 1991; Candela et al., 1999; Hoffmann and Poorter, 2002). In some species with prominent veins, it has been shown that potential quantum yield of photosystem II (F_v/F_m) reaches a maximum before maximal leaf expansion is reached and that, in general, differentiation processes of major veins precede mesophyll growth and differentiation (Walter et al., 2004). Vein development and differentiation have been well characterized, and depend on an intricate interplay of various phytohormones, including auxin gradients (Mattsson et al., 2003; Rolland-Lagan, 2008). However, the cues for mesophyll differentiation remain unknown.

On the basis of mutant analyses in *Arabidopsis*, the bundle sheath, a chlorenchymatic cell layer tightly surrounding the vasculature, has been hypothesized to play an important role in mesophyll differentiation (Kinsman and Pyke, 1998; Streatfield et al., 1999; González-Bayón et al., 2006). A class of mutants displaying a reticulated leaf phenotype was reported that is characterized by a well-differentiated bundle sheath with intact chloroplasts and a mesophyll tissue that is pale to white with fewer cells and/or disrupted chloroplasts (Kinsman and Pyke, 1998).

George Rédei described the first reticulated mutant *reticulata* (*re*) and used it as a visible marker in genetic crosses (Rédei and Hironyo, 1964). Several additional reticulated mutants have been implicated in leaf differentiation since *cab*

¹ To whom correspondence should be addressed. E-mail aweber@uni-duesseldorf.de, fax +49-211-8113706, tel. +49-211-8112347.

© The Author 2012. Published by the Molecular Plant Shanghai Editorial Office in association with Oxford University Press on behalf of CSPB and IPPE, SIBS, CAS.

doi:10.1093/mp/sss045, Advance Access publication 24 April 2012

Received 4 September 2011; accepted 22 March 2012

underexpressed 1 (cue1) (Li et al., 1995), *venosa 1–6 (ven1-6)* (Berná et al., 1999), and *differential development of vascular associated cells 1 (dov1)* (Kinsman and Pyke, 1998).

Ven2 is allelic to *re* (Berná et al., 1999). The gene affected in *re* was positionally cloned and shown to encode a chloroplast-localized membrane protein (González-Bayón et al., 2006). The function of the gene product remains unknown to date. *Re* mutants have a reticulated leaf phenotype with fewer mesophyll cells compared to wild-type (González-Bayón et al., 2006).

Cue1 is defective in the phosphoenolpyruvate–phosphate translocator (PPT) of the chloroplast envelope membrane (Streatfield et al., 1999). Initially, it was hypothesized to be ‘a cell-specific positive regulator linking light and intrinsic developmental programs in *Arabidopsis* leaf mesophyll cells’ (Li et al., 1995). Similarly to *re*, *cue1* mutants have fewer mesophyll cells that contain a lower number of chloroplasts (Li et al., 1995). PPT imports phosphoenolpyruvate (PEP) into the chloroplasts, where it is used as the major precursor of the shikimic acid pathway (Schmid and Amrhein, 1995; Fischer et al., 1997; Knappe et al., 2003; Voll et al., 2003; Tzin and Galili, 2010). The *cue1* mutant contains lower amounts of aromatic amino acids, has a deregulated amino acid metabolism, and contains reduced levels of shikimate-derived secondary metabolites (Streatfield et al., 1999; Voll et al., 2003). The *cue1* phenotype could be rescued by supplementation with all three aromatic amino acids tryptophan, tyrosine, and phenylalanine. It was concluded that the *cue1* phenotype is caused by either decreased supply of aromatic amino acids or by a lack of aromatic amino acid-derived metabolites (Streatfield et al., 1999; Voll et al., 2003). On the basis of these results, it was hypothesized that a chloroplast-derived signal, that is dependent on either PEP or its metabolic products, causes the reticulated *cue1* leaf phenotype (Streatfield et al., 1999).

A different genetic screen for altered leaf phenotypes yielded the reticulated *venosa 1 to 6 (ven1-6)* mutant series (Berná et al., 1999). In addition to *ven2*, which is allelic to *re*, *ven3* and *ven6* were recently identified at the molecular level (Mollá-Morales et al., 2011). Much like *cue1*, the *ven3* and *ven6* gene products are involved in amino acid metabolism. *Ven3* and *ven6* encode subunits of the carbamoyl phosphate synthase required for ornithine to citrulline conversion during arginine biosynthesis (Mollá-Morales et al., 2011). *Ven3* and *ven6* are single-copy genes in *A. thaliana*, *ven3* and *ven6* are not fully penetrant, leading to basal levels of arginine synthesis and survival of the plant (Mollá-Morales et al., 2011). The pale to white mesophyll tissue with fewer mesophyll cells and chloroplasts is credited to disturbed protein biosynthesis. It was concluded that arginine is vital for correct leaf development (Mollá-Morales et al., 2011). In line with these findings, mutants that are defective in ribosomal protein subunits and are consequently disturbed in protein biosynthesis also show reticulated leaves (Horiguchi et al., 2011).

Dov1, another reticulated mutant, was discovered in a screen to identify genes that are involved in the differential development of vasculature associated tissues (Kinsman and Pyke, 1998). All mutants identified in this screen possessed a reticulate leaf structure (Kinsman and Pyke, 1998). The phenotype is specific to leaves, and not seen in cotyledons and other aerial tissues. The *dov1* mutation is nuclear recessive and is allelic neither to *cue1* nor to *re* (Kinsman and Pyke, 1998). *Dov1*, which is in the Enkheim-2 (En-2) background, was not positionally cloned to date (Kinsman and Pyke, 1998).

Recently, interest in the bundle sheath has been renewed, since it is a key tissue in C_4 photosynthesis but little understood in C_3 plants (Kobayashi et al., 2009; Aubry et al., 2011). In this study, to gain insight into the role of the bundle sheath during mesophyll differentiation in C_3 plants, *dov1* mutant plants were analyzed with regard to their growth patterns, metabolism, hormone levels, and hormone responses. The affected gene was positionally cloned and identified as ATase2, one of three isoenzymes that catalyze the first step of purine biosynthesis. Since *re*, *cue1*, *ven2*, *ven3*, *ven6*, and *dov1* are now positionally cloned, the *signaling hypothesis* and the *limited supply hypothesis* are critically discussed.

RESULTS

Plant Growth Rates and Photosynthetic Capacity

Dov1 plants were smaller than wild-type controls (Kinsman and Pyke, 1998). *Dov1* was also variable in its penetrance, depending on environmental conditions and plant age (Kinsman and Pyke, 1998; our own observations). We investigated this phenotype in detail by simultaneous growth and photosynthetic performance measurements under controlled conditions.

Growth was determined by means of non-destructive image analysis estimating the rosette size from consecutive images taken at the same time each day. The relative growth rate (RGR) was calculated to assess the relative increase of projected leaf area from observation point to observation point (Hoffmann and Poorter, 2002; Jansen et al., 2009). Simultaneously, the ratio of variable fluorescence to maximum fluorescence (F_v/F_m) of dark-adapted leaves was measured to investigate changes in photosynthetic capacity with regard to energy transfer in intact photosystem II reaction centers.

At the beginning of the monitoring period, the plants were 21 day old (21 d post germination, dpG) (Figure 1A and Supplemental Table 1). At this time, the leaf area of the En-2 plants was 2.5 times larger than the area of the mutants, with 0.91 cm² (S.E. 0.07 cm²) compared to 0.36 cm² (S.E. 0.03 cm²). The reticulated pale phenotype was fully apparent at this point. After 9 d of constant monitoring, the difference in size increased to about 4.3-fold, comparing *dov1* to En-2 (1.73 cm²; S.E. 0.11 and 7.40 cm²; S.E. 0.46 cm², respectively).

The RGR of En-2 significantly exceeded that of *dov1* at three observation points, namely from 21 to 22, 23 to 24, and 25 to 27 dpG. Both RGR changes of mutants and wild-type changed simultaneously (Figure 1B and Supplemental Table 2).

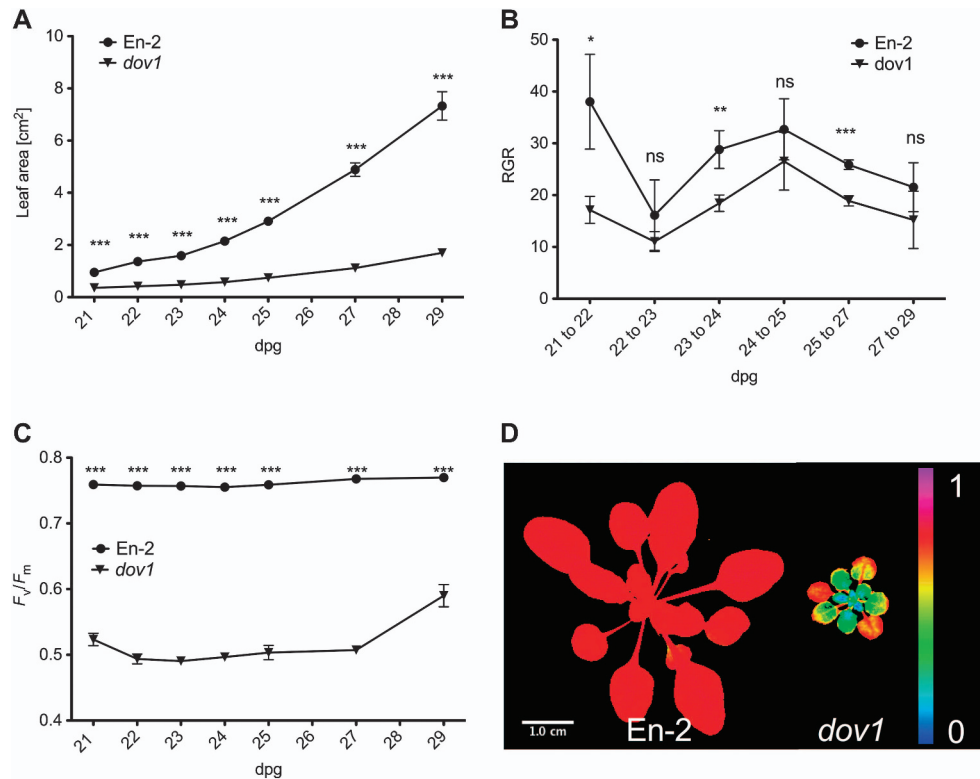


Figure 1. Growth Kinetics and Photosynthetic Activity of En-2 and *dov1* Plants.

(A) Total leaf area of En-2 and *dov1* from 21 to 29 d post germination (dpg) ($n > 15$).

(B) Relative growth rate (RGR) along 9 d of observation. RGR refers to two subsequent monitoring points.

(C) Photosynthetic capacity as indicated by F_v/F_m from 21 to 29 dpg.

(D) False color image of En-2 and *dov1* plants displaying F_v/F_m ratios. Plants shown are representative for plants of 29 dpg ($n > 15$). Error bars represent S.E. Asterisks indicate significance levels.

The photosynthetic performance as characterized by F_v/F_m of En-2 plants at all detected growth stages stayed at a constant level of about 0.78 (Figure 1C and Supplemental Table 1). Compared to wild-type, the *dov1* plants had significantly decreased F_v/F_m values of about 0.50 during the first seven observation days, indicating lower photosynthetic performance. During the time of observation, the overall F_v/F_m of *dov1* plants increased significantly from 0.50 at 25 dpg to 0.59 at 29 dpg by 18% ($p = 0.0001$).

The photosynthetic performance of *dov1* varied not only over time, but also with leaf age (Figure 1D). Within a rosette, the oldest leaves (the outermost whirl of the rosette) had a potential photosynthetic performance almost comparable to wild-type as indicated by the close to red color of the F_v/F_m false color image. Intermediately aged leaves appeared mostly green in the pseudo-fluorescence images, while the youngest leaves are green to blue in color. In younger *dov1* leaves, the photosynthetic performance was highest at the leaf tip. In En-2, the F_v/F_m ratio was constant across different leaf ages of the plant rosette (Figure 1D), which also appeared uniformly green to the eye (Figure 2D). The *dov1* parameters were consistent with the visible phenotype: the youngest leaves (with the exception of cotyledons) displayed the most severe

visible phenotype, while older leaves turned green (Figures 2D, 3B, and 3D). The decreased photosynthetic capacity is also reflected by the lowered chlorophyll contents of *dov1* compared to En-2 (Supplemental Figure 1A).

Map-Based Cloning of *dov1* and Testing for Allelism

The key to interpreting these and previous results (Kinsman and Pyke, 1998) was to identify the affected gene in *dov1*. *Dov1* is an EMS-mutant in the En-2 background. To map the *dov1* mutation, it was crossed into the Col-0 background. Thirty-five PCR markers were inferred from known polymorphisms between *Landsberg erecta* (Ler) and Col-0 accessions that were extracted from the TAIR database (Swarbreck et al., 2008), and tested for applicability to an En-2/Col-0 cross. 15 suitable markers covering all chromosomes were used for rough mapping of the mutation. Eighty-eight plants with the *dov1* phenotype were selected from the F2-progeny of the mapping cross. They were analyzed using the above-mentioned PCR markers. The mutation was linked to both markers 12 and 19 on the lower arm of chromosome four (Figure 2A). The two additional markers M45 and M47 were established on the lower arm of chromosome four (see Supplemental Table 3 for markers used). The mapping population

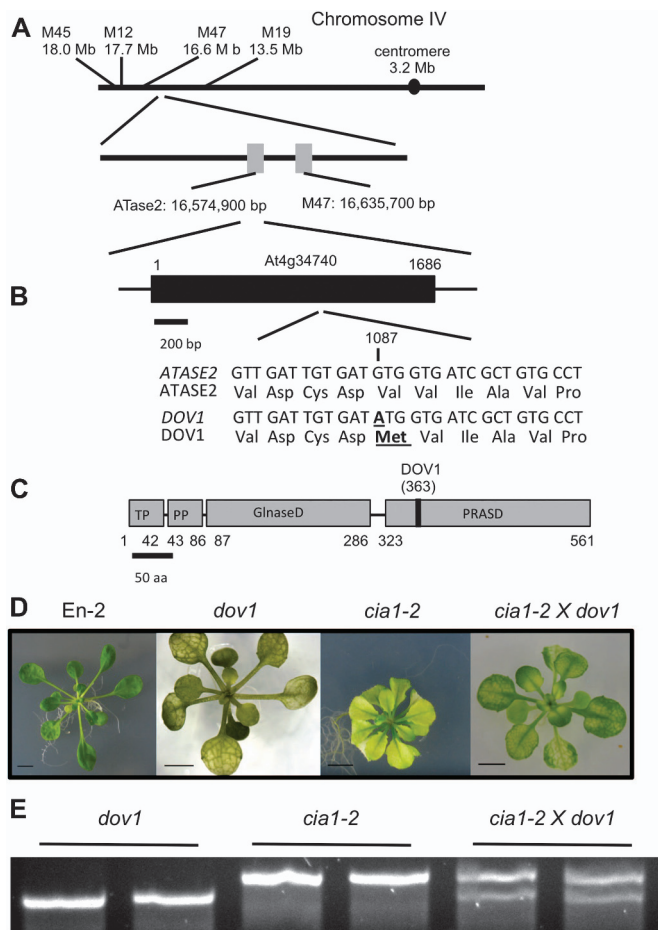


Figure 2. Mapping of *DOV1* and Allelism Test.

(A) Map-based cloning of *dov1* and markers used.
 (B) The single exon gene is mutated at position 1087, giving rise to a valine-to-methionine exchange.
 (C) Schematic domain structure of ATase2. cTP, predicted chloroplast transit peptide; PP, pro-peptide; GlnaseD, glutaminase domain; PRASD, PRA synthase domain.
 (D) Four-week-old plants of En-2, *dov1*, *cia1-2*, and F1-offspring of *cia1-2 x dov1*. The F1-cross showed the reticulated pattern of both *cia1* and *dov1* parent plants.
 (E) Gel electrophoresis of PCR products on genomic DNA with marker 12. The homozygous state of *dov1* and *cia1-2* is indicated by smaller and larger band sizes, respectively. The heterozygous state of F1 plants of a cross between *cia1-2* and *dov1* (*cia1-2 x dov1*) is indicated by two bands.

was extended to 556 F₂-plants, resulting in recombination frequencies of 8.80% for marker 19, 6.94% for marker 12, 9.84% for marker 45, and 0.27% for marker 47.

This mapping population yielded an interval with 60 genes (data not shown), which was screened for candidate genes. The interval included the gene *At4g34740*, which encodes for ATase2. The ATase2 mutants *cia1-1*, *cia1-2*, and *atd2*, which are all in the Col-0 background, show phenotypes similar to *dov1* (Hung et al., 2004; van der Graaff et al., 2004). Hence, we hypothesized that *dov1* might be defective in ATase2 function.

To test whether the *At4g34740* gene was indeed mutated, the coding sequence including the 5'-UTR and 3'-UTR of *At4g34740* was isolated from *dov1* and wild-type by PCR and sequenced. A comparison of the sequences from the En-2 wild-type and *dov1* revealed a substitution of a single nucleotide from guanine to adenine. This mutation causes an amino acid exchange from valine to methionine at position 363 (Val363Met) relative to the start codon of the ATase2 protein (Figure 2B and 2C). Val363 was either conserved or changed conservatively in all organism tested (Supplemental Figure 2). The mutation in *dov1* was located in the PRA synthase domain (PRASD) of the ATase2 protein (Figure 2C).

The genetic mapping results were confirmed by testing *dov1* and *cia1-2* for allelism. *Cia1-2* in the Col-0 background was crossed with *dov1* in the En-2 background. The resulting F₁-generation showed the same phenotype as *dov1* and *cia1-2* (Figure 2D). The F₁-offspring was heterozygous with regard to En-2 and Col-0, as indicated by the simple sequence length polymorphism marker (SSLP-marker) 12 (Figure 2E). The test confirmed that *dov1* is an allele of *cia1-2*, and thereby a new allele of all known ATase2 mutant lines.

Mutant *dov1* ATase2 Has No Activity *In Vitro*

ATases are ubiquitous enzymes that catalyze the first step in the *de novo* purine biosynthesis. ATases convert glutamine into glutamate by amination of 5-phosphoribosyl-1-pyrophosphate (PRPP) to 5-phospho-ribosylamine (PRA) (Zrenner et al., 2006). PRA is used to produce purine nucleotides in a series of downstream enzymatic reactions (Zrenner et al., 2006) (Figure 4). To test whether the *dov1* mutation in a conserved residue of the PRASD (Figure 2C and Supplemental Figure 2) affected the function of ATase2, the ATase2 and the mutated DOV1 protein were heterologously expressed in *E. coli*. The ATases of all eukaryotic and many prokaryotic organisms are N-terminally flanked by a pro-peptide (PP) that is auto-catalytically cleaved to give rise to a cysteine residue. The SH-group of the cysteine acts in the catalytic site of the glutaminase domain (Walsh et al., 2007). Additionally, the *Arabidopsis* ATase2 carries a chloroplast-targeting transit peptide (cTP) at its N-terminal end (Emanuelsson et al., 2000; Hung et al., 2004; Walsh et al., 2007). To express both the mutated DOV1 and the wild-type ATase2 enzymes in *E. coli*, the predicted cTP was eliminated and the 11 amino acids of the PP were kept in order not to interfere with the enzyme's function (Walsh et al., 2007). Both proteins were expressed with and without hexahistidine tags for detection and purification. The tagged wild-type enzyme showed no activity (data not shown). We hence chose the untagged, recombinantly expressed ATases from wild-type and *dov1* for further analyses. Total protein was isolated, and the enzyme activity was tested in a two-step assay (Walsh et al., 2007). A reaction lacking the substrate PRPP was used as a negative control. Unlike the wild-type enzyme, the DOV1 enzyme showed no activity above background level in all experiments (Figure 5A).

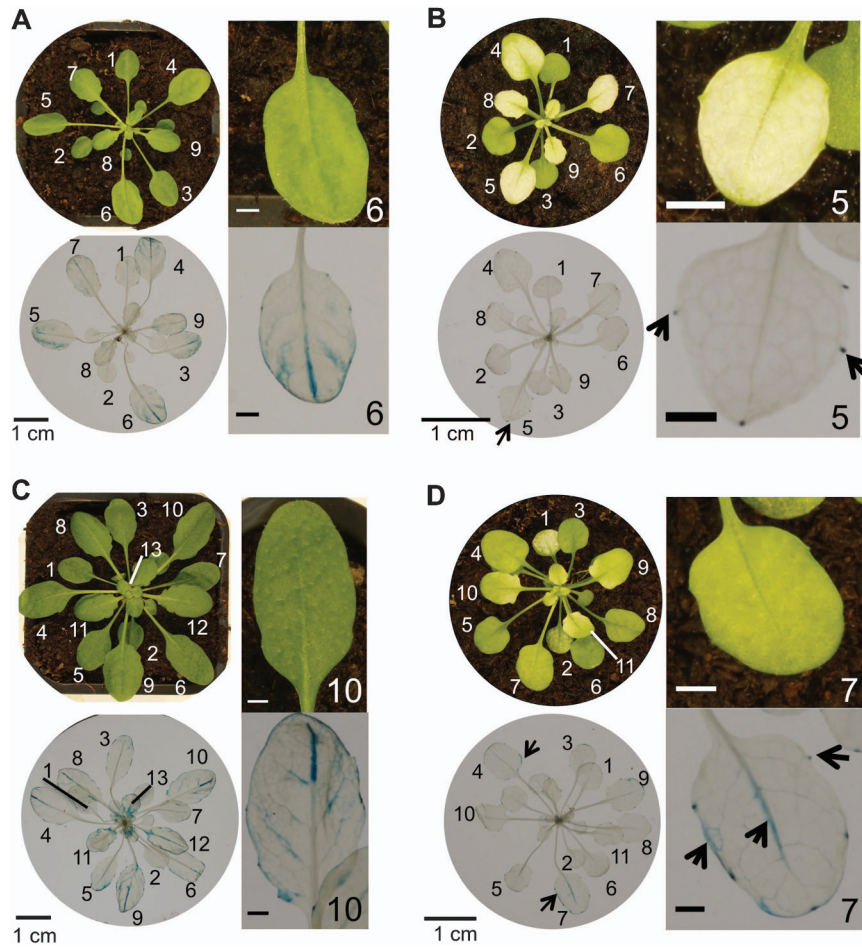


Figure 3. Cytokinin (ARR5–GUS) (A, B) and Auxin (DR5–GUS) (C, D) reporter Assays in Wild-Type and *dov1* Background of 8-Week-Old Plants, Respectively.

Pictures were taken before and immediately after GUS staining. The number of leaves are arranged from oldest to youngest leaves beginning with 1. The scale-up of single representative leaves is shown right to the whole rosettes. The scale bar in the magnification corresponds to 0.2 cm.

ATase Activity Is Reduced in *dov1* Plants

Three different ATase isoforms are present in *A. thaliana* of which all three are expressed to different degrees in leaf tissue (Hung et al., 2004; Supplemental Figures 2 and 3). To assess whether total ATase activity was lowered in *dov1* or whether the two other isoforms ATase1 and ATase3 were able to compensate for ATase2, ATase activity was determined *in planta*. En-2 plants had a significantly 1.8-fold higher total ATase activity than *dov1* (Figure 5B).

Metabolite Profiling of *dov1*

Purine levels were decreased in the *dov1* allele *cia1* (Hung et al., 2004). To assess whether the defect in ATase2 also had a direct influence on the amino acids involved in purine biosynthesis, we profiled amino acids and organic acids by gas chromatography coupled to mass spectrometry (GC–MS).

The steady-state levels of seven amino acids were significantly increased in the *dov1* mutant: α -alanine (2.5-fold), asparagine (21.3-fold), aspartate (4.1-fold), glycine (2.3-fold),

proline (11.5-fold), lysine (6.6-fold), and ornithine (15.8-fold) (Figure 6). Inorganic phosphate was also increased (12.9-fold). The biological variation in metabolite contents was higher in *dov1* compared to wild-type (Figure 6 and Supplemental Table 4). All other tested metabolites, including all carbohydrates, were not significantly changed in their relative amounts between wild-type and *dov1* (Supplemental Table 4).

Quantitation of Cytokinin Levels and Complementation with Cytokinin

Because cytokinins are purine-derived (Mok and Mok, 2001; Smith and Atkins, 2002) and play crucial roles in leaf development (DeMason, 2005; Efroni et al., 2010), cytokinin levels were profiled in *dov1*.

The total content of all determined cytokinins, namely free cytokinin bases and conjugated forms, were significantly decreased by 22% ($p = 0.0363$) in *dov1* compared to the wild-type (Figure 7B and Supplemental Table 5).

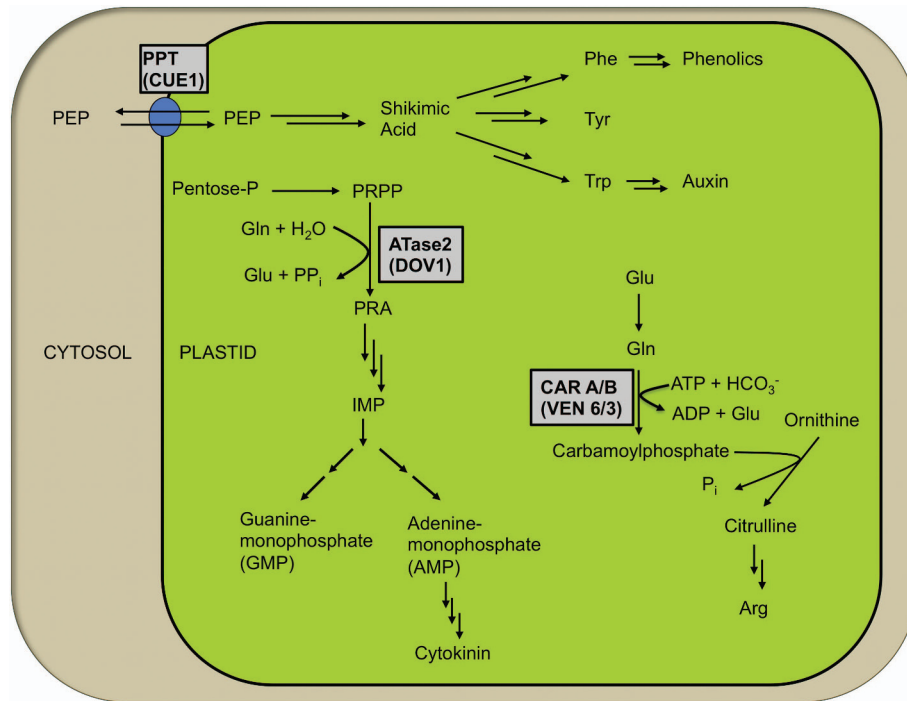


Figure 4. Schematic Overview of the Metabolic Pathways of the Reticulated Mutants *dov1*, *ven3/6*, and *cue1*.

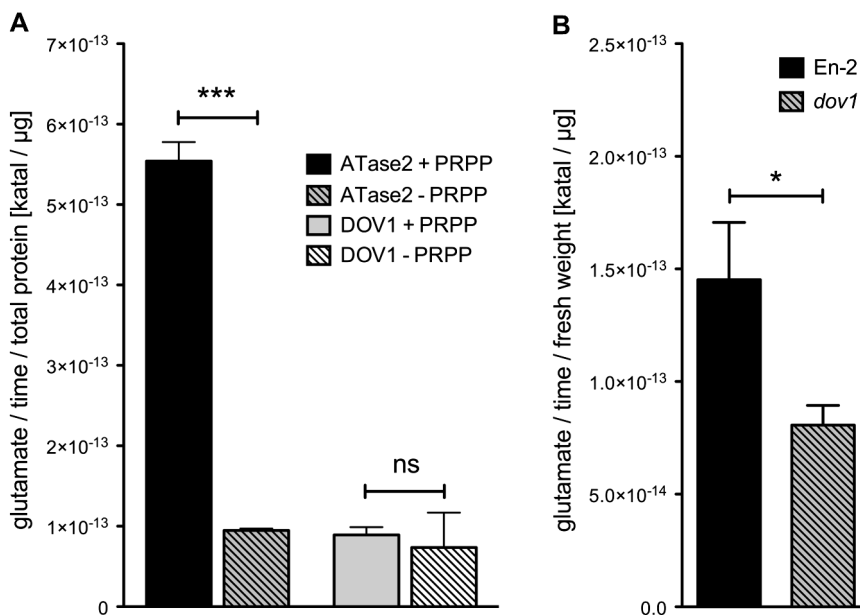


Figure 5. Enzymatic Activity of ATase and the Mutated DOV1-Protein.

(A) Enzymatic activity of heterologously expressed ATase2 and DOV1 in *E. coli* ($n = 4$). (B) *In planta* total ATase activity in En-2 and *dov1* ($n = 5$).

While total iP-cytokinins and *cis*-zeatin cytokinins were at the same level in wild-type and *dov1*, total *trans*-zeatin cytokinins were significantly decreased by 34% in the mutant compared to the wild-type ($p = 0.0035$). The *trans*-zeatin cytokinins represented the vast majority of cytokinins in both wild-type and *dov1* (Figure 7B and Supplemental Table 5). Some conjugated *trans*-zeatin cytokinins were higher in the

wild-type than in *dov1*, and vice versa (Supplemental Table 5). The conjugated derivatives are considered deactivated (Mok and Mok, 2001; Bajguz and Piotrowska, 2009).

Despite overall lowered cytokinin contents in *dov1*, the free active cytokinin base *trans*-zeatin (tZ) was increased in *dov1* (2.9-fold). *Cis*-zeatin (cZ) and N⁶-(Δ^2 -isopentyl)adenine (iP) levels were indistinguishable between *dov1* and wild-type

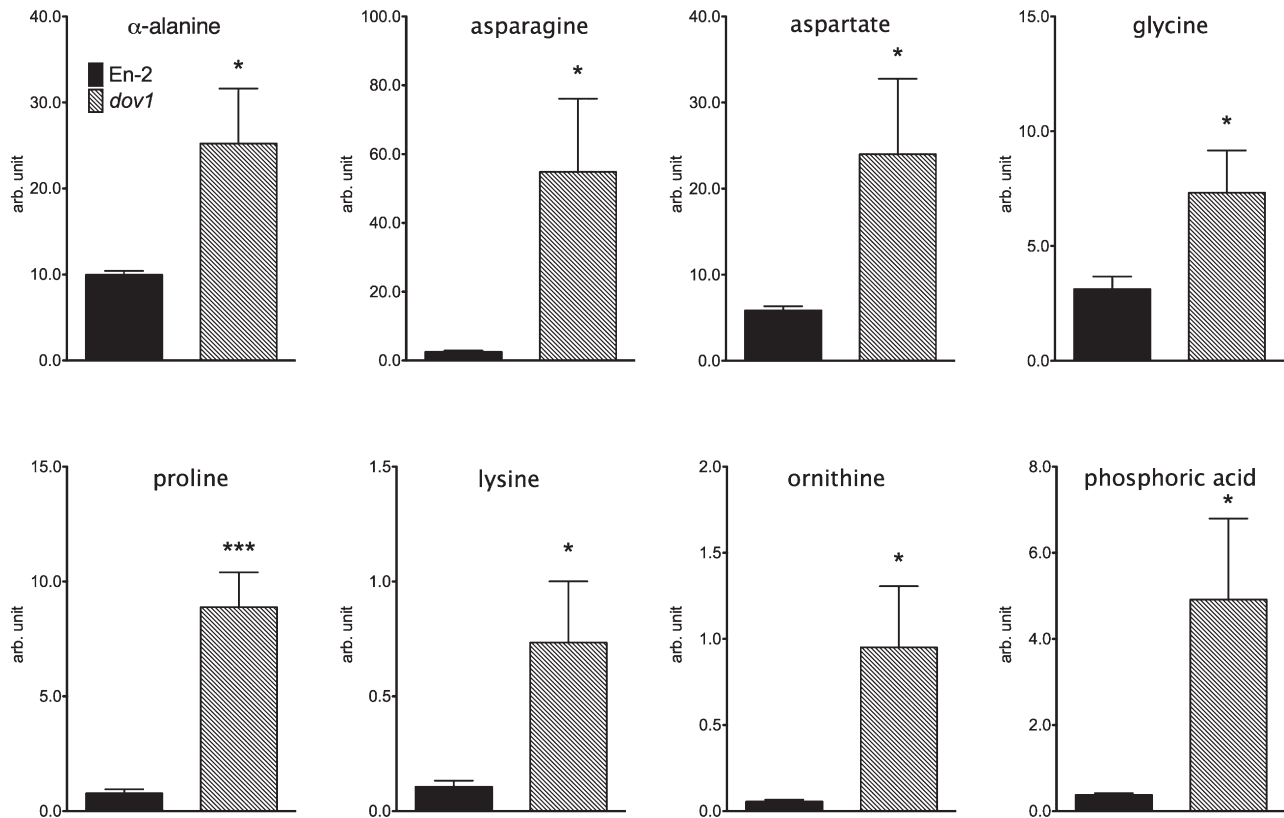


Figure 6. Significantly Changed Steady-State Metabolite Levels in 7-Week-Old En-2 and *dov1* Rosettes before Transition to Budding and Flowering.

Plants were grown under 12-h/12-h light/dark cycle at $100 \mu\text{E m}^{-2} \text{s}^{-1}$. Samples were taken in the middle of the light period. Arbitrary units (arb. units) are shown. The error bars represent S.E. Asterisks indicate significance levels. $n(\text{En-2}) = 8$, $n(\text{dov1}) = 7$.

(Figure 7C and Supplemental Table 5). The latter three cytokinin bases are considered as the physiological active forms, with *cZ* having the weakest activity (Leonard et al., 1969; Schmitz et al., 1972a, 1972b; Matsubara, 1980; Mok and Mok, 2001). *tZ* and *iP* are the major forms in *Arabidopsis* (Sakakibara, 2006).

To test whether the *dov1* phenotype could be restored by exogenous application of cytokinin, plants were biochemically supplemented with the cytokinin derivative 6-benzylaminopurine (BA) (Figure 7A). However, the BA feeding had an effect on neither the En-2 nor the *dov1* plants at very low concentrations (0.001 and 0.01 nM). With increasing concentrations of BA (0.1 and 1.0 nM), the wild-type plants showed stunted growth with pale leaves, and the *dov1* plants did not re-green. Thus, above a threshold level of external BA application, the phenotypes of wild-type and *dov1* resembled each other. Both mutant line and wild-type showed toxic syndromes with increasing BA concentration. Similar results were found when growing *cia1-2* on cytokinin plates (Hung et al., 2004).

A Cytokinin Reporter but Not an Auxin Reporter Responds Differentially in *dov1*

Cytokinins and auxin play crucial roles in leaf development (DeMason, 2005; Rolland-Lagan, 2008; Efroni et al., 2010).

To investigate whether these phytohormones displayed distinct physiological patterns in *dov1*, we crossed the mutant into ARR5-GUS (D'Agostino et al., 2000) and DR5-GUS reporter lines (Ulmasov et al., 1997; Robles et al., 2010), respectively. Eight-week-old rosettes with wild-type and *dov1* morphology were selected for GUS staining. Plants were documented immediately before and after GUS staining (Figure 3).

Leaves of every developmental stage from wild-type plants harboring the ARR5-GUS construct showed GUS activity (Figure 3A). Both younger (e.g. leaf 8) and older leaves showed less activity than intermediately aged leaves (leaves 3, 4, 5, 6, and 7). The latter showed a higher GUS activity around the major veins, on the leaf lamina with emphasis at the distal tip part, at the leaf margins, and at the hydathodes (Figure 3A). The GUS staining in *dov1* background at all leaf developmental stages was restricted to the hydathodes of the leaf teeth, as indicated by the arrows (Figure 3B). These GUS staining patterns coincided with neither pale nor green areas of the leaves (Figure 3B).

The DR5-GUS reporter in the wild-type background displayed activity in all rosette leaves (Figure 3C). Older leaves showed less activity than younger and intermediately aged

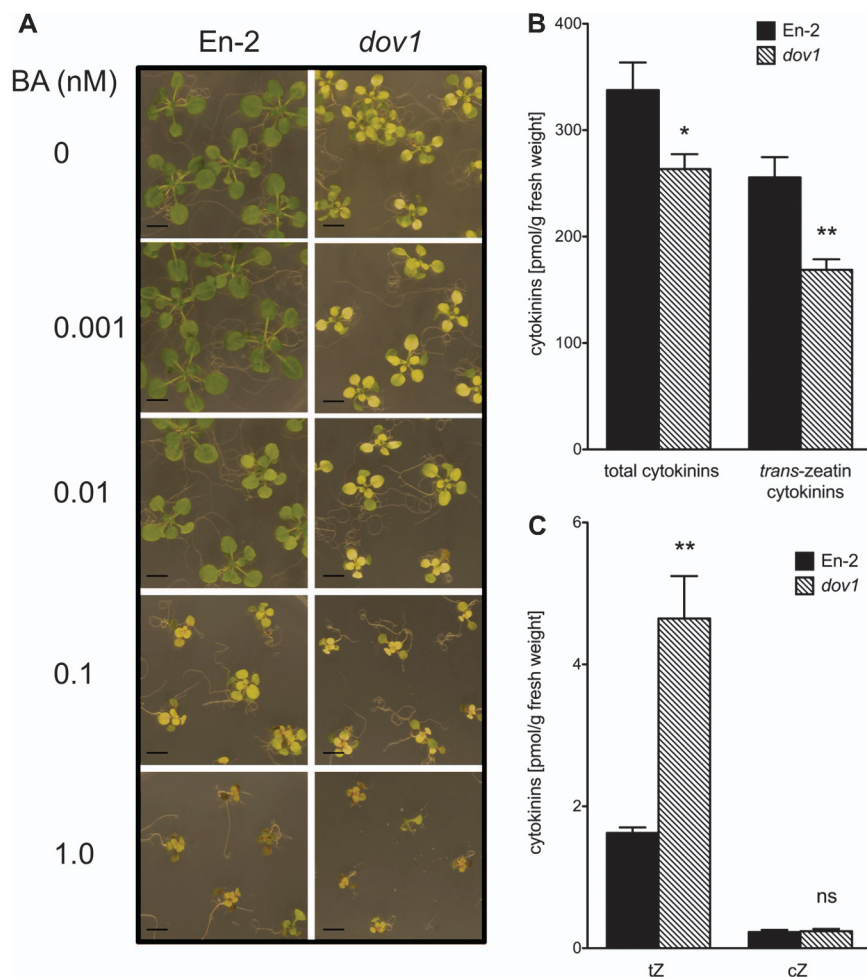


Figure 7. Exogenous Application of Cytokinin to En-2 and *dov1* Plants and Cytokinin Concentrations of En-2 and *dov1*.

(A) Three-week-old En-2 and *dov1* plants exogenously supplemented with increasing concentrations of 6-benzylaminopurine (BA) in 1 MS medium. The scale bar corresponds to 0.5 cm.

(B) Levels of total cytokinins and total *trans*-zeatin cytokinin derivatives of 7-week-old En-2 and *dov1* plants.

(C) Levels of the active cytokinins *trans*-zeatin (tZ) and *cis*-zeatin (cZ) of 7-week-old En-2 and *dov1* plants. Error bars represent S.E. Stars indicate significance levels ($n = 5$). Plants for (A), (B), and (C) were grown under 12-h/12-h light/dark cycle at $100 \mu\text{E m}^{-2} \text{s}^{-1}$.

leaves, with restriction of the GUS staining to the leaf margin (e.g. leaf 2). In intermediately aged leaves (leaves 5–12), the GUS staining is primarily found around the major veins, the leaf margins, and the hydathodes of the leaf teeth (Figure 3C). Younger, emerging leaves showed GUS staining at the leaf basis and around the margins. GUS activity in the *dov1* background was generally less pronounced than in the wild-type control (Figure 3D). Whereas the oldest leaves (e.g. leaf 1) only showed staining at the hydathodes, intermediately aged leaves (e.g. leaves 4, 7, and 9) displayed GUS staining along the leaf margin, the hydathodes, and the major veins as indicated by the arrows (Figure 3D). The staining in the youngest emerging leaves was restricted to the leaf tip. In comparison to the cytokinin reporter ARR5–GUS in the *dov1* background, the DR5–GUS reporter showed a generally more intense staining and had an intermediate phenotype when compared to the wild-type.

DISCUSSION

To understand the role of *dov1* in leaf development and organization, the mutant was phenotypically and metabolically characterized, and the defective gene identified.

Dov1 Is Defect in the ATase2 Gene Product

The defective gene in the *dov1* mutant was unknown, although it is one of the hallmark mutants used in analyzing internal leaf development (Kinsman and Pyke, 1998). The reason for this was probably its genetic background in En-2.

We mapped *dov1* to the gene locus At4g34740, which encodes ATase2, the enzyme catalyzing the first step of purine biosynthesis. In the mutant enzyme, valine at position 363 was exchanged to methionine (Figure 2B and 2C). *In vitro*, no enzyme activity was measured. Hence, Val363 is essential for the enzyme function (Figure 5A). The valine residue is conserved in

ATase2 proteins from bacteria to plants (Supplemental Figure 2). *A. thaliana* harbors three loci for ATases: ATase1, 2, and 3. Since the purine biosynthesis is essential, viability of *dov1* depends on the activities of ATases 1 and 3 (Supplemental Figures 3 and 4). Therefore, we tested to what degree total ATase activity is lowered in *dov1*. *Dov1* showed a 1.8-fold decrease in total ATase activity in its aerial tissues (Figure 5B). This decrease was due to the defect of the mutated ATase2 enzyme because the mutated recombinant protein DOV was not functional *in vitro* (Figure 5A).

The previously reported ATase2 mutants *cia1-1*, *cia1-2*, and *atd2* showed phenotypes similar to *dov1* with pale and reticulated leaves (Hung et al., 2004; van der Graaff et al., 2004). Crosses of *dov1* with *cia1-2* confirmed allelism. This indicates that the two domains of ATase2 (Figure 2C, 2D and 2E) might act in *cis*, not in *trans*, although this hypothesis awaits testing in the future. The mutation in *dov1* was localized to the PRA domain while the mutations in the *cia* mutants were localized to the glutaminase domain (Hung et al., 2004). These tests confirmed that *dov1* is a new allele of ATase2.

Consequences of Limited Purine Availability for Primary Leaf Metabolism

Mutants in ATase2 had lower purine levels in leaves compared to wild-type (Hung et al., 2004; van der Graaff et al., 2004). The mutants could be complemented with externally applied purines (Hung et al., 2004), which showed that a functional salvage pathway was capable of supplying almost enough purines to the leaf. Despite the fact that the ATase2 mutants *cia1* (Hung et al., 2004), *atd2* (van der Graaff et al., 2004), and *dov1* (Kinsman and Pyke, 1998) grew much more slowly compared to wild-type (Figure 1A and 1B), the growth reduction was not strong enough to permit the formation of small, but green leaves with intact chloroplasts.

Within the leaf, not only purine levels were changed (Hung et al., 2004), but also several proteinogenic amino acids and inorganic phosphate had altered steady-state levels (Figure 6 and Supplemental Table 4). The increased levels of the purine building blocks aspartate and glycine (Zrenner et al., 2006) might result from the decreased purine production in *dov1* (Figures 4 and 6). The increased amounts of N-rich amino acids asparagine, lysine, and the asparagine precursor ornithine, as well as the increase in alanine, aspartate, and glycine, and the overall stable level of carbohydrates might be a consequence of an altered C/N-homeostasis. Purines bind considerable amounts of nitrogen (Reinbothe and Mothes, 1962; Smith and Atkins, 2002). Lowered leaf purine levels may lead to an increased flux of N into the biosynthesis of N-rich amino acids as a compensatory effect. The increase in proline may indicate that the plants perceive the lack of purines as a stress that activates a generic stress response, such as the accumulation of proline (Delauney and Verma, 1993; Parry et al., 2005; Verdoy et al., 2006; Lea et al., 2007; Nicotra et al., 2011). Since the metabolites determined were either at the same level or higher in *dov1* compared to

the wild-type, these metabolites were not causal for the phenotype.

Cytokinins and Altered Growth Patterns of *dov1* Leaves

We and others observed that *dov1* mutants, depending on their growth density on MS-plates, the day/night-cycle length as well as their age, varied considerably for the extent of reticulation and paleness of their leaves (data not shown; Kinsman and Pyke, 1998). The growth screens revealed a constant growth rate of both *dov1* and wild-type plants, with a generally lower rate of *dov1* (Figure 1A and 1B).

Photosynthetic performance and the visible phenotype of *dov1* not only varied with plant age, but also showed an age-related pattern. Older *dov1* leaves displayed almost normal photosynthetic performance, while younger leaves had their highest performance at the leaf tip. In wild-type, the photosynthetic performance was independent of leaf age (Figures 1D).

The age-related differences did not correlate with the expression patterns of the ATases because they did not vary in expression during leaf development (public data from the *Arabidopsis* efp browser; Supplemental Figure 3; Winter et al., 2007).

Purines are precursors of cytokinins (Mok and Mok, 2001), which are known to drive the mitotic events in plants (Redig et al., 1996), and are abundant in meristematic tissues (Nishinari and Syono, 1980; Ascough et al., 2009). It was shown that purine biosynthesis genes have a stronger expression in mitotically active tissues, and are thus involved in cell division (Zhang et al., 1996; van der Graaff et al., 2004; Zrenner et al., 2009).

To assess the role of cytokinins in *dov1* leaf development, cytokinin levels in leaves were determined and the response to active cytokinins (Shtratnikova and Kulaeva, 2008) was assessed by the ARR5-GUS-promoter activity in the *dov1* background. Total cytokinin levels were decreased in *dov1* compared to wild-type (Figure 7B), reflecting the decreased total ATase activity (Figure 5B). ATase1 and 3 apparently did not fully compensate the cytokinin biosynthesis. The active tZ, however, was increased in *dov1*. tZ is reported to be the most active cytokinin, while the conjugated derivatives are assumed to be non-active (Mok and Mok, 2001; Bajguz and Piotrowska, 2009). While the cytokinin response, as indicated by the ARR5-GUS reporter, was found on the leaf lamina, around the midvein, the margins, and the hydathodes of younger wild-type leaves, the cytokinin response in *dov1* was restricted to the hydathodes of each rosette leaf. The cause of this restriction is likely due to the lack of supply with purines caused by the inactivity of ATase2. The activity in hydathodes as a site of high transpiration might reflect an accumulation of cytokinins from the transpiration stream (Aloni et al., 2005). At the hydathodes, the active cytokinins do not contribute to leaf growth. Furthermore, exogenous cytokinin application reverted neither the *dov1* nor the *cia1-2* phenotype (Hung et al.,

2004). The cytokinin even had toxic effects to both wild-type and mutant plants (Figure 7A).

Auxin responsiveness in the *dov1* background is not as restricted as the cytokinin response (Figure 3B and 3D). In some leaves, there was still a response to auxin at the leaf margins and in the major veins (Figure 3D). Thus, the responsiveness seemed to be intermediary. The responsiveness, even if limited compared to the wild-type, is likely to be explained by the fact that auxin biosynthesis is not directly dependent upon purines (Zhao, 2010) (Figure 4). However, it is tempting to speculate that the lowered auxin activity in the *dov1* background compared to the wild-type is an indirect consequence of altered cytokinin levels, particularly since it is known that there is an extensive crosstalk between auxin and cytokinin action (Moubayidin et al., 2009).

Taken together, limited supply provided a likely explanation for the large phenotypic plasticity in the *dov1* mutant (this publication; Kinsman and Pyke, 1998; Hung et al., 2004; van der Graaff et al., 2004). The plasticity was not due to inherent variability of the genotype because the standard errors for all parameters measured under controlled conditions were small (Figures 1A–1C, 5, 6, and 7, and Supplemental Tables 1, 2, 4, and 5). Phenotypic variability may result from conditions that decrease purine demand. Mature leaves with only few dividing cells possibly require less *de novo* purine biosynthesis. Thus, decreased supply of purines, such as in old mature leaves as compared to young leaves, permitted old leaves to turn green.

The Basis of Reticulated Leaf Patterning

The basis of the reticulated leaf pattern in *dov1*, *re*, *cue1*, *ven3*, and *ven6* has not been addressed conclusively to date. Strikingly, all functionally characterized reticulated mutants are affected in primary metabolic genes and consequently in primary metabolism (Streatfield et al., 1999; Mollá-Morales et al., 2011; this work), although all were initially hypothesized in a *signaling hypothesis* to encode regulatory components important for mesophyll differentiation.

In none of the reticulated mutants reported to date has the effect on plant hormones been investigated. Since cytokinin is involved in cell division and auxin in overall leaf differentiation (DeMason, 2005; Rolland-Lagan, 2008; Efroni et al., 2010), the response to these hormones were tested in this study, using reporter constructs.

Cue1 is involved in shikimic acid and thus aromatic amino acid biosynthesis, *ven3* and *ven6* are involved in arginine synthesis, and *dov1* contributes to *de novo* purine synthesis. All of the affected pathways localize to the plastid (Figure 4). Despite their co-localization, the pathways are not directly connected, because, apart from the fact that the purine-based metabolite ATP is the general energy currency of the cell, they do not share substrates or products (Figure 4). Moreover, metabolites, which would require products of all three pathways for their synthesis, have not been described to date. While this does not exclude the hypothesis of a signaling molecule as the cause of

the phenotype (Kinsman and Pyke, 1998; Streatfield et al., 1999), it makes it at least unlikely.

Analysis of the *ven3* and *ven6* mutants and experiments using arginine biosynthesis inhibitors in pea leaves conclusively demonstrated that leaves turn white in the absence of arginine (Turner and Mitchell, 1985). *Ven3* and *ven6* mutants have decreased levels of arginine and/or citrulline (Mollá-Morales et al., 2011). Unlike *re* and *cue1*, *ven3* and *ven6* have already been considered metabolic rather than signaling mutants (Mollá-Morales et al., 2011).

Cue1 is a full knockout of one of two plastidial phosphoenolpyruvate–phosphate translocators (PPTs), which feed the plastid-localized shikimic acid pathway with phosphoenolpyruvate and all reactions depending on it. The steady-state amino acid levels reflect an imbalance of non-aromatic to aromatic amino acids, a decrease in phenylalanine, and a reduced flux into phenylalanine-derived secondary metabolites (Streatfield et al., 1999; Voll et al., 2003). However, transgenic wild-type-like plants in the *cue1* background harboring an overexpressed plastidic enzyme, which produces PEP, had overall diminished aromatic amino acids (Voll et al., 2003; Weber et al., 2004). Thus, it has been argued that the affected aromatic amino acids biosynthesis is not simply the cause of the *cue1* phenotype (Voll et al., 2003). Rather, a metabolic signal involved in leaf development was postulated.

Unlike the *ven3* and *ven6* mutations, which are leaky, *cue1* is a complete knockout of PPT1. Survival of the plants is likely dependent on a second transporter with identical transport function but different expression domains (Knappe et al., 2003). Taking the plant's response to a *cue1* knockout (Streatfield et al., 1999; Voll et al., 2003) into account, the limited phenylalanine and its derived secondary metabolites availability may well be the primary cause of the reduced cell number and paleness in *cue1*. This is supported by the fact that ribosomal protein mutants with limited protein biosynthesis also show reduced cell number (Horiguchi et al., 2011).

Similarly to *ven3*, *ven6*, and *cue1*, the *dov1* gene product ATase2 also provides a metabolite that is essential to the cell, purine. Similarly to *cue1*, the absence of *dov1* can be partially compensated by additional isoforms. Hence, purines can still be produced *in planta* by ATase1 and 3, albeit they are not highly expressed in leaf tissue (Supplemental Figure 3). The decreased total cytokinin levels and the restricted cytokinin response pattern in *dov1* are likely to be seen as a lack of supply with purines.

The joint interpretation of the three mutants *ven3/6*, *cue1*, and *dov1* with apparent defects in mesophyll but healthy bundle sheaths points to limited supply of essential metabolites as the main reason for the reticulate phenotypes observed. Why, then, are the bundle sheaths and the leaf margins green or at least greener than the remainder of the leaf? Vein and therefore bundle sheath differentiation predates mesophyll differentiation (Kinsman and Pyke, 1998). Hence, if a limited supply of metabolites is given, either in the leaf itself or from other organs, the early differentiating tissues can properly form,

while tissues differentiating later are more likely to be limited. In true leaves, only the early differentiating bundle sheaths and nearby tissues are green, while mesophyll is bleached (Li et al., 1995; Kinsman and Pyke, 1998; González-Bayón et al., 2006; Mollá-Morales et al., 2011). The transport of primary metabolites via the vasculature is likely sufficient to deliver enough metabolites to allow greening of the tissue. Vascular-located transporters for amino acids (Frommer et al., 1995) and putative vascular purine transporters (Maurino et al., 2006) have been identified.

The detailed analysis of photosynthetic performance in *dov1* supports this hypothesis. Once cell division stops and leaves mature, the supply of purines from other sources may again be sufficient to allow re-greening of the older leaves (Figure 2D, 3B and 3D) and recovery of photosynthetic performance (Figure 1C and 1D). This indicates that mesophyll cell aberrations are not permanent. The nature of the *dov1* mutant supports a *limited supply* rather than a *signaling hypothesis* as the reason for reticulation. The mapping of the remaining reticulated mutants and the elucidation of *re* function will be instrumental in distinguishing between these two hypotheses.

METHODS

Plant Material, General Growth Conditions, and Plant Lines

Arabidopsis thaliana plants were grown under controlled conditions in climate chambers. The day/night cycle was chosen as 12 h light and 12 h with a photosynthetically active radiation of $100 \mu\text{E m}^{-2} \text{s}^{-1}$. Temperature was set to 22°C during light, and 18°C during the dark period. In special experiments, the deviant growth conditions are indicated.

Seeds were surface-sterilized with chlorine gas in a desiccator as previously described (Desfeux et al., 2000), spotted on solid 1 Murashige and Skoog (MS)-medium with vitamins containing 0.8% (*w/w*) plant agar (Murashige and Skoog, 1962), and stratified at 4°C for 4 d. All plant material was germinated and grown in 1 MS medium.

The *dov1*-seeds were obtained from our laboratory stock, whereas the EMS-mutant *cia1-2* was obtained from the European Arabidopsis Stock Centre. DR5-GUS- and ARR5-GUS-plants were kindly provided by Rüdiger Simon and Nicole Stahl (Institute of Developmental Genetics, Heinrich-Heine-University, Düsseldorf). DR5 is an artificial promoter that reacts to changed auxin perception (Ulmasov et al., 1997; Robles et al., 2010). ARR5-GUS indicates changing cytokinin patterns (D'Agostino et al., 2000).

DR5-GUS and ARR5-GUS-reporter lines were crossed into *dov1*. The F₂-generation of both the DR5-GUS and the ARR5-GUS-crosses with *dov1* was visually selected for the *dov1* and En-2 phenotype. *Dov1* and En-2 phenotypic plants of the F₂ generation were screened via GUS staining for changing GUS-patterns.

Mapping of *dov1*

Dov1, which is an EMS-mutant in the En-2 background, was crossed into the Col-0 background in order to map the mutant. Map-based cloning was adapted and performed as previously described (Jander et al., 2002). Thirty-five PCR markers were inferred from known polymorphisms between Ler and Col-0, and tested for applicability to an En-2/Col-0 cross. Four markers did not yield PCR products under the conditions used and 16 markers were not different between Col-0 and En-2. 15 suitable markers covering all chromosomes were used for rough mapping of the mutation (see Supplemental Table 5 for all markers used). Eighty-eight plants with the *dov1* phenotype were selected from the F₂-progeny of the mapping cross. They were analyzed using the 15 PCR markers. The mutation was linked to both markers 12 and 19 on the lower arm of chromosome four. The additional markers M45 and M47 were established on the lower arm of chromosome four. Recombination was calculated to test for the linkage of loci. The mapping population was extended to 556 F₂-plants resulting in recombination frequencies of 8.80% for marker 19, 6.94% for marker 12, 9.84% for marker 45, and 0.27% for marker 47. This mapping population yielded an interval with 60 candidate genes, which was screened for candidate genes. The interval included the gene At4g34740.

The candidate *Atase2* was isolated by PCR-based means with the forward primer 5'-aacggaatcaaatcttagtaaatagag-3' binding in the 5'-UTR, and the reverse primer 5'-aaattgaccccaaaccaaa-3' binding in the 3'-UTR. After cloning into the blunt end vector pJET1.2 (Fermentas, Thermo Scientific, Germany), the PCR product was sequenced. The described base pair exchange at position 1087 in *dov1* was detected.

The recombination frequency (RF) in percentage represents the ratio of recombinant gametes with regard to the *dov1* locus to the total number of gametes. The RF was calculated by the equation $RF = ((2 \cdot n(\text{Col-0}) + 1 \cdot n(\text{het}) + 0 \cdot n(\text{En-2})) / 2n)$, where $n(\text{Col-0})$ is the number of plants homozygous for the Col-0 allele, $n(\text{het})$ is the number of plants for the heterozygous plants, $n(\text{En-2})$ is the number of plants for the En-2 allele, and n is the total number of plants analyzed. A $RF \geq 50\%$ was regarded as free recombination, namely as unlinked loci, whereas a $RF < 50\%$ was considered as coupled recombination, namely linked loci.

GUS Staining

GUS-staining was performed as previously described (Mattsson et al., 2003). Whole rosettes of 6-week-old *dov1* and En-2 plants were vacuum infiltrated with the GUS staining solution (0.1 M NaH₂PO₄, pH 7.0; 10 mM Na₂EDTA; 0.5 M Sodium-Ferricyanide K₃[Fe(CN)₆]; 0.5 M Sodium-Ferrocyanide K₄[Fe(CN)₆] × 3H₂O, 0.1% Triton X-100, and 1 mM 5-bromo-4-chloro-3-indoyl-beta-GlcUA (Inalco Spa)). The samples were incubated at 37°C for 24 h. Hereafter, the staining solution was removed, and fixation solution was added (50% (m/m) Ethanol, 5% (m/m) Glacial acetic acid, and 3.7% (m/m)

Formaldehyde). The samples stored in the staining solution were incubated for 10 min at 65°C. The leaf tissue was destained three times after removal of the fixation solution with 80% (m/m) Ethanol. Pictures were taken with a digital camera (Canon D40).

Biochemical Complementation with Cytokinin

After 7 d of growth on MS-plates, seedlings were transferred onto MS-plates containing different concentrations of 6-benzylaminopurine (0.001, 0.01, 0.1, and 1 nM BA). Plants were monitored for an additional 2 weeks. Pictures were taken with a digital camera (Canon D40).

Metabolite Profiling

Dov1 and En-2-plants were grown under controlled conditions in a light chamber in a 12-h/12-h light/dark cycle (100 $\mu\text{E m}^{-2} \text{s}^{-1}$) on 1 MS medium (Murashige and Skoog, 1962), and transferred on soil after 2 weeks. Whole rosettes from 7-week-old *dov1* and En-2 plants were harvested before flowering, and snap-frozen in liquid nitrogen. Polar metabolites from homogenized rosette material samples (~50 mg) were extracted using a chloroform-methanol extraction protocol (Fiehn, 2006). The extraction mix was vortexed for 20 s, shaken in a rotating device for 6 min at 4°C, then centrifuged for 2 min at 20 000 g. 1 ml of the supernatant was vortexed for 10 s. 100 μl of this extract was lyophilized and derivatized using methoxyamine hydrochloride in pyridine followed by N-methyl-N-(trimethylsilyl)-fluoroacetamide (MSFTA) treatment (Fiehn, 2006).

The relative amounts of 15 amino acids, 12 carbohydrates, eight carboxylic acids, shikimate, and phosphate were determined as described previously (Gowik et al., 2011).

Cytokinin Quantification

Plants were grown as described for metabolite profiling. Five rosettes of each En-2 and *dov1* rosettes were pooled. Five replicates of each pooled sample were used for cytokinin quantification. For endogenous cytokinins analysis, extraction and purification were performed according to the method previously described (Novák et al., 2003). Levels of cytokinins were quantified by ultra-performance liquid chromatography-electrospray tandem mass spectrometry (UPLC_MS/MS) (Novák et al., 2008).

Chlorophyll Determination

Plants were grown for 5 weeks under 16-h/8-h light/dark at 100 $\mu\text{E m}^{-2} \text{s}^{-1}$ at 22°C/18°C. Plant material was harvested in the middle of the light period, snap-frozen in liquid nitrogen, and homogenized by grinding in a mortar. The fresh weight was determined and the chlorophyll concentration was determined as described previously (Porra et al., 1989).

Enzymatic Assays

The enzyme activity assay was conducted as previously reported (Kim et al., 1996; van der Graaff et al., 2004) and

adapted to *Arabidopsis thaliana*. Aerial parts of 6-week-old plants, grown on MS-plates, were harvested before budding and flowering, processed, and used for measuring ATase activity. 0.8 g of *Arabidopsis* plant material were homogenized in 1 ml of plant extraction buffer (pH 6.8, 1 mM EDTA, 1 mM MgCl_2 , 5 mM glutathione, 20 mM DTT, 0.1 mM phenylmethanesulfonyl fluoride (PMSF), 0.1 mM 4-(2-Aminoethyl) benzenesulfonyl fluoride hydrochloride (AEBSF), 2 μM Pepstatin A). The homogenate was centrifuged for 1 min at 20 000 g. The supernatant was desalted using Zeba™ Spin Desalting Columns (Thermo Scientific). The flow-through was used for the activity assay.

ATase activity was determined by measuring the PRPP-dependent formation of glutamate from glutamine. 50 μl aliquots of plant extract were assayed in 100 μl of assay I reaction mix, which contained in final concentrations: 5 mM MgCl_2 , 3 mM PRPP, 20 mM NaF, 5 mM glutamine. Control assays were performed by adding glutamine but no PRPP. The reactions were stopped at 100°C for 3 min in a water bath. Glutamate concentration was measured using the glutamate dehydrogenase method (Messenger and Zalkin, 1979). The assay contained 50 mM Tris-HCl, pH 8.0, 267 $\mu\text{l ml}^{-1}$ H_2O , 3 mM 3-Acetylpyridine adenine dinucleotide (APAD), 133 $\mu\text{l ml}^{-1}$ assay I reaction mix, 4 U ml^{-1} glutamate dehydrogenase. The formation of APADH⁺ was monitored in a plate reader at 363 nm (Biotek plate reader KC4 with supplied software). PRPP-dependent activity was calculated by subtracting the PRPP-independent activity.

GROWSCREEN FLUORO Analysis of Growth, Fluorescence, and Phenotypic Properties

Batches of plants grown on soil were analyzed for growth and phenotypic properties by using the GROWSCREEN FLUORO phenotyping platform as described previously (Jansen et al., 2009). 15 or more biological replicates were used for each of the En-2 plants and the *dov1* mutants. The phenotyping set-up uses a fluorescence-imaging camera together with an illumination head to automatically acquire images of every plant inside the batches placed in the set-up (Jansen et al., 2009). Plants were imaged non-invasively for a period of 9 d at the same time every day. For calculation of F_v/F_m , plants were dark-adapted for 30 min. Based on the acquired images, image analysis provided several datasets for each mutant and wild-type plants, including the RGR, and efficiency of photosystem II (Walter et al., 2007; Jansen et al., 2009). The RGR was calculated using the equation $\text{RGR} = (\text{mean of } \ln(A_2) - \text{mean of } \ln(A_1))/t_2 - t_1$ (Hoffmann and Poorter, 2002; Jansen et al., 2009).

Statistical Analysis

Statistical significance was assessed by the Student's *t*-test. Probability values (*p*) < 0.05 were considered being significant. One star indicates *p* < 0.05, two stars indicate *p* < 0.01, and three stars indicate *p* < 0.0001. The standard error of the mean (S.E.) is indicated in all plots, if not indicated otherwise.

Alignment of Protein Sequences

Protein Atase2 sequences of different organisms were inferred from publicly available databases. Alignment of the sequences was performed with CLC Genomic Workbench (www.clcbio.com). The settings were chosen as follows: default alignment, gap open cost 10, gap extension 1, and end gap cost as any other.

SUPPLEMENTARY DATA

Supplementary Data are available at *Molecular Plant Online*.

FUNDING

This work was funded by grants of the Deutsche Forschungsgemeinschaft (DFG CRC 590 to A.P.M.W. and iRTG 1525 to A.P.M.W. and A.W.) and by Grant No. KAN200380801 to M.S.

ACKNOWLEDGMENTS

We thank Prof. Dr. Rüdiger Simon and Dr. Yvonne Stahl for providing us with the ARR5-GUS and DR5-GUS reporter lines. We appreciate technical assistance by Katrin L. Weber and Elisabeth Klemp with GC/MS-analysis of metabolites and by Manuel Wagner with plate growth assays. We thank Steffen Köhler for assistance with photographic documentation of the reporter lines and the cytokinin plate assays. No conflict of interest declared.

REFERENCES

- Aloni, R., Langhans, M., Aloni, E., Dreieicher, E., and Ullrich, C.I. (2005). Root-synthesized cytokinin in *Arabidopsis* is distributed in the shoot by the transpiration stream. *J. Exp. Bot.* **56**, 1535–1544.
- Ascough, G.D., et al. (2009). Hormonal and cell division analyses in *Watsonia lepidota* seedlings. *J. Plant Physiol.* **166**, 1497–1507.
- Aubry, S., Brown, N.J., and Hibberd, J.M. (2011). The role of proteins in C₃ plants prior to their recruitment into the C₄ pathway. *J. Exp. Bot.* **62**, 3049–3059.
- Bajguz, A., and Piotrowska, A. (2009). Conjugates of auxin and cytokinin. *Phytochem.* **70**, 957–969.
- Berná, G., Robles, P., and Micol, J.L. (1999). A mutational analysis of leaf morphogenesis in *Arabidopsis thaliana*. *Genetics.* **152**, 729–742.
- Candela, H., Martínez-Laborda, A., and Micol, J.L. (1999). Venation pattern formation in *Arabidopsis thaliana* vegetative leaves. *Dev. Biol.* **205**, 205–216.
- D'Agostino, I.B., Deruère, J., and Kieber, J.J. (2000). Characterization of the response of the *Arabidopsis* response regulator gene family to cytokinin. *Plant Physiol.* **124**, 1706–1717.
- Delauney, A.J., and Verma, D.P.S. (1993). Proline biosynthesis and osmoregulation in plants. *Plant J.* **4**, 215–223.
- DeMason, D.A. (2005). Auxin-cytokinin and auxin-gibberellin interactions during morphogenesis of the compound leaves of pea (*Pisum sativum*). *Planta.* **222**, 151–166.
- Desfeux, C., Clough, S.J., and Bent, A.F. (2000). Female reproductive tissues are the primary target of *Agrobacterium*-mediated transformation by the *Arabidopsis* floral-dip method. *Plant Physiol.* **123**, 895–904.
- Efroni, I., Eshed, Y., and Lifschitz, E. (2010). Morphogenesis of simple and compound leaves: a critical review. *Plant Cell.* **22**, 1019–1032.
- Emanuelsson, O., Nielsen, H., Brunak, S., and von Heijne, G. (2000). Predicting subcellular localization of proteins based on their N-terminal amino acid sequence. *J. Mol. Biol.* **300**, 1005–1016.
- Fiehn, O. (2006). Metabolite profiling in *Arabidopsis*. In *Arabidopsis* Protocols, 2nd edn, Salinas, J., and Sanchez-Serrano, J.J., eds. Methods in Molecular Biology ser. (Totowa, NJ: Humana Press), pp. 439–447.
- Fischer, K., et al. (1997). A new class of plastidic phosphate translocators: a putative link between primary and secondary metabolism by the *phosphoenolpyruvate/phosphate* antiporter. *Plant Cell.* **9**, 453–462.
- Frommer, W.B., Hummel, S., Unseld, M., and Ninnemann, O. (1995). Seed and vascular expression of a high-affinity transporter for cationic amino acids in *Arabidopsis*. *Proc. Natl Acad. Sci. U S A.* **92**, 12036–12040.
- González-Bayón, R., et al. (2006). Mutations in the *RETICULATA* gene dramatically alter internal architecture but have little effect on overall organ shape in *Arabidopsis* leaves. *J. Exp. Bot.* **57**, 3019–3031.
- Gowik, U., Brautigam, A., Weber, K.L., Weber, A.P.M., and Westhoff, P. (2011). Evolution of C₄ photosynthesis in the genus *Flaveria*: how many and which genes does it take to make C₄? *Plant Cell.* **23**, 2087–2105.
- Hoffmann, W.A., and Poorter, H. (2002). Avoiding bias in calculations of relative growth rate. *Ann. Bot.* **90**, 37–42.
- Horiguchi, G., et al. (2011). Differential contributions of ribosomal protein genes to *Arabidopsis thaliana* leaf development. *Plant J.* **65**, 724–736.
- Hung, W.F., Chen, L.J., Boldt, R., Sun, C.W., and Li, H.M. (2004). Characterization of *Arabidopsis* glutamine phosphoribosyl pyrophosphate amidotransferase-deficient mutants. *Plant Physiol.* **135**, 1314–1323.
- Jander, G., Norris, S.R., Rounsley, S.D., Bush, D.F., Levin, I.M., and Last, R.L. (2002). *Arabidopsis* map-based cloning in the post-genome era. *Plant Physiol.* **129**, 440–450.
- Jansen, M., et al. (2009). Simultaneous phenotyping of leaf growth and chlorophyll fluorescence via GROWSCREEN FLUORO allows detection of stress tolerance in *Arabidopsis thaliana* and other rosette plants. *Funct. Plant Biol.* **36**, 902–914.
- Kim, J.H., Krahn, J.M., Tomchick, D.R., Smith, J.L., and Zalkin, H. (1996). Structure and function of the glutamine phosphoribosylpyrophosphate amidotransferase glutamine site and communication with the phosphoribosylpyrophosphate site. *J. Biol. Chem.* **271**, 15549–15557.
- Kinsman, E.A., and Pyke, K.A. (1998). Bundle sheath cells and cell-specific plastid development in *Arabidopsis* leaves. *Development.* **125**, 1815–1822.
- Knappe, S., Löttgert, T., Schneider, A., Voll, L., Flügge, U.I., and Fischer, K. (2003). Characterization of two functional *phosphoenolpyruvate/phosphate translocator* (*PPT*) genes in *Arabidopsis*

- AtPPT1 may be involved in the provision of signals for correct mesophyll development. *Plant J.* **36**, 411–420.
- Kobayashi, H., Yamada, M., Taniguchi, M., Kawasaki, M., Sugiyama, T., and Miyake, H.** (2009). Differential positioning of C₄ mesophyll and bundle sheath chloroplasts: recovery of chloroplast positioning requires the actomyosin system. *Plant Cell Physiol.* **50**, 129–140.
- Lea, P.J., Sodek, L., Parry, M.A.J., Shewry, R., and Halford, N.G.** (2007). Asparagine in plants. *Ann. Appl. Biol.* **150**, 1–26.
- Leonard, N.J., Hecht, S.M., Skoog, F., and Schmitz, R.Y.** (1969). Cytokinins: synthesis, mass spectra, and biological activity of compounds related to zeatin. *Proc. Natl Acad. Sci. U S A.* **63**, 175–182.
- Li, H.M., Culligan, K., Dixon, R.A., and Chory, J.** (1995). *CUE1*: a mesophyll cell-specific positive regulator of light-controlled gene expression in *Arabidopsis*. *Plant Cell.* **7**, 1599–1610.
- Matsubara, S.** (1980). Structure-activity-relationships of cytokinins. *Phytochem.* **19**, 2239–2253.
- Mattsson, J., Ckurshumova, W., and Berleth, T.** (2003). Auxin signaling in *Arabidopsis* leaf vascular development. *Plant Physiol.* **131**, 1327–1339.
- Maurino, V.G., Grube, E., Zielinski, J., Schild, A., Fischer, K., and Flügge, U.I.** (2006). Identification and expression analysis of twelve members of the nucleobase-ascorbate transporter (NAT) gene family in *Arabidopsis thaliana*. *Plant Cell Physiol.* **47**, 1381–1393.
- Messenger, L.J., and Zalkin, H.** (1979). Glutamine phosphoribosylpyrophosphate amidotransferase from *Escherichia coli*: purification and properties. *J. Biol. Chem.* **254**, 3382–3392.
- Mok, D.W.S., and Mok, M.C.** (2001). Cytokinin metabolism and action. *Ann. Rev. Plant Physiol. Plant Mol. Biol.* **52**, 89–118.
- Mollá-Morales, A., et al.** (2011). Analysis of *ven3* and *ven6* reticulate mutants reveals the importance of arginine biosynthesis in *Arabidopsis* leaf development. *Plant J.* **65**, 335–345.
- Moubayidin, L., Di Mambro, R., and Sabatini, S.** (2009). Cytokinin–auxin crosstalk. *Trends Plant Sci.* **14**, 557–562.
- Murashige, T., and Skoog, F.** (1962). A revised medium for rapid growth and bio assays with tobacco tissue cultures. *Physiol. Plant.* **15**, 473–497.
- Mustroph, A., et al.** (2009). Profiling transcriptomes of discrete cell populations resolves altered cellular priorities during hypoxia in *Arabidopsis*. *Proc. Natl Acad. Sci. U S A.* **106**, 18843–18848.
- Nicotra, A.B., et al.** (2011). The evolution and functional significance of leaf shape in the angiosperms. *Func. Plant Biol.* **38**, 535–552.
- Nishinari, N., and Syono, K.** (1980). Identification of cytokinins associated with mitosis in synchronously cultured tobacco cells. *Plant Cell Physiol.* **21**, 383–393.
- Novák, O., Hauserová, E., Amakorová, P., Doležal, K., and Strnad, M.** (2008). Cytokinin profiling in plant tissues using ultra-performance liquid chromatography–electrospray tandem mass spectrometry. *Phytochem.* **69**, 2214–2224.
- Novák, O., Tarkowski, P., Tarkowska, D., Doležal, K., Lenobel, R., and Strnad, M.** (2003). Quantitative analysis of cytokinins in plants by liquid chromatography–single–quadrupole mass spectrometry. *Anal. Chim. Acta.* **480**, 207–218.
- Parry, M.A.J., Flexas, J., and Medrano, H.** (2005). Prospects for crop production under drought: research priorities and future directions. *Ann. Appl. Biol.* **147**, 211–226.
- Porra, R.J., Thompson, W.A., and Kriedemann, P.E.** (1989). Determination of accurate extinction coefficients and simultaneous equations for assaying chlorophyll a and chlorophyll b extracted with four different solvents: verification of the concentration of chlorophyll standards by atomic absorption spectroscopy. *Biochim. Biophys. Acta.* **975**, 384–394.
- Pyrke, K.A., Marrison, J.L., and Leech, R.M.** (1991). Temporal and spatial development of the cells of the expanding first leaf of *Arabidopsis thaliana* (L.) heynh. *J. Exp. Bot.* **42**, 1407–1416.
- Rédei, G.P., and Hironyo, Y.** (1964). Linkage studies. *Arabidopsis Information Service.* **1**, 9–10.
- Redig, P., Shaul, O., Inzé, D., Van Montagu, M., and Van Onckelen, H.** (1996). Levels of endogenous cytokinins, indole-3-acetic acid and abscisic acid during the cell cycle of synchronized tobacco BY-2 cells. *FBS Lett.* **391**, 175–180.
- Reinbothe, H., and Mothes, K.** (1962). Urea, ureides, and guanidines in plants. *Annu. Rev. Plant Biol.* **13**, 129–150.
- Robles, P., et al.** (2010). The *RON1/FRY1/SAL1* gene is required for leaf morphogenesis and venation patterning in *Arabidopsis*. *Plant Physiol.* **152**, 1357–1372.
- Rolland-Lagan, A.-G.** (2008). Vein patterning in growing leaves: axes and polarities. *Curr. Opin. Genet. Dev.* **18**, 348–353.
- Sakakibara, H.** (2006). Cytokinins: activity, biosynthesis, and translocation. *Ann. Rev. Plant Biol.* **57**, 431–449.
- Schmid, J., and Amrhein, N.** (1995). Molecular organization of the shikimate pathway in higher plants. *Phytochem.* **39**, 737–749.
- Schmitz, R.Y., Skoog, F., Bock, R.M., Leonard, N.J., and Hecht, S.M.** (1972a). Comparison of cytokinin activities of naturally occurring ribonucleases. *Phytochem.* **11**, 1603–1610.
- Schmitz, R.Y., Skoog, F., Playtis, A.J., and Leonard, N.J.** (1972b). Cytokinins: synthesis and biological activity of geometric and position isomers of zeatin. *Plant Physiol.* **50**, 702–705.
- Shtatnikova, V.Y., and Kulaeva, O.N.** (2008). Cytokinin-Dependent Expression of the ARR5::GUS Construct during Transgenic *Arabidopsis* Growth. *Russian Journal of Plant Physiology* **55**, 756–764.
- Smith, P.M.C., and Atkins, C.A.** (2002). Purine biosynthesis: big in cell division, even bigger in nitrogen assimilation. *Plant Physiol.* **128**, 793–802.
- Streatfield, S.J., et al.** (1999). The *phosphoenolpyruvate/phosphate translocator* is required for phenolic metabolism, palisade cell development, and plastid-dependent nuclear gene expression. *Plant Cell.* **11**, 1609–1621.
- Swarbreck, D., et al.** (2008). The *Arabidopsis* Information Resource (TAIR): gene structure and function annotation. *Nucl. Acids Res.* **36**, D1009–D1014.
- Turner, J.G., and Mitchell, R.E.** (1985). Association between symptom development and inhibition of ornithine carbamoyltransferase in bean leaves treated with phaseolotoxin. *Plant Physiol.* **79**, 468–473.
- Tzin, V., and Galili, G.** (2010). New insights into the shikimate and aromatic amino acids biosynthesis pathways in plants. *Mol. Plant.* **3**, 956–972.

- Ulmasov, T., Murfett, J., Hagen, G., and Guilfoyle, T.J. (1997). Aux/IAA proteins repress expression of reporter genes containing natural and highly active synthetic auxin response elements. *Plant Cell*. **9**, 1963–1971.
- van der Graaff, E., et al. (2004). Molecular analysis of 'de novo' purine biosynthesis in solanaceous species and in *Arabidopsis thaliana*. *Front. Biosci.* **9**, 1803–1816.
- Verdoy, D., De la Peña, T.C., Redondo, F.J., Lucas, M.M., and Pueyo, J.J. (2006). Transgenic *Medicago truncatula* plants that accumulate proline display nitrogen-fixing activity with enhanced tolerance to osmotic stress. *Plant Cell Environ.* **29**, 1913–1923.
- Voll, L.M., et al. (2003). The phenotype of the *Arabidopsis cue1* mutant is not simply caused by a general restriction of the shikimate pathway. *Plant J.* **36**, 301–317.
- Walsh, T.A., et al. (2007). Chemical genetic identification of glutamine phosphoribosylpyrophosphate amidotransferase as the target for a novel bleaching herbicide in *Arabidopsis*. *Plant Physiol.* **144**, 1292–1304.
- Walter, A., et al. (2007). Dynamics of seedling growth acclimation towards altered light conditions can be quantified via GROWSCREEN: a setup and procedure designed for rapid optical phenotyping of different plant species. *New Phytol.* **174**, 447–455.
- Walter, A., Rascher, U., and Osmond, B. (2004). Transitions in photosynthetic parameters of midvein and interveinal regions of leaves and their importance during leaf growth and development. *Plant Biol.* **6**, 184–191.
- Weber, A.P.M., Schneidereit, J., and Voll, L.M. (2004). Using mutants to probe the *in vivo* function of plastid envelope membrane metabolite transporters. *J. Exp. Bot.* **55**, 1231–1244.
- Winter, D., Vinegar, B., Nahal, H., Ammar, R., Wilson, G.V., and Provart, N.J. (2007). An 'Electronic Fluorescent Pictograph' browser for exploring and analyzing large-scale biological data sets. *PLoS One.* **2**, 1–12.
- Zhang, K., Letham, D.S., and John, P.C.L. (1996). Cytokinin controls the cell cycle at mitosis by stimulating the tyrosine dephosphorylation and activation of p34^{cdc2}-like H1 histone kinase. *Planta*. **200**, 2–12.
- Zhao, Y.D. (2010). Auxin biosynthesis and its role in plant development. In *Annual Review of Plant Biology*, Vol. 61, Merchant S. Briggs W.R. and Ort D., eds. (Palo Alto, California: Town), pp. 49–64.
- Zrenner, R., et al. (2009). A functional analysis of the pyrimidine catabolic pathway in *Arabidopsis*. *New Phytol.* **183**, 117–132.
- Zrenner, R., Stitt, M., Sonnewald, U., and Boldt, R. (2006). Pyrimidine and purine biosynthesis and degradation in plants. *Annu. Rev. Plant Biol.* **57**, 805–836.